

Theoretical Possibilities of Controlling the Cooling Rate in the Heat Treatment of Cast Iron with Water Mist

Piotr Stręk 

AGH University of Krakow, Faculty of Foundry Engineering, Mickiewicza 30, 30-059 Krakow, Poland
e-mail: piotr@ledavi.com

© 2024 Author. This is an open access publication, which can be used, distributed and reproduced in any medium according to the Creative Commons CC-BY 4.0 License requiring that the original work has been properly cited.

Received: 14 October 2024/Accepted: 2 December 2024 /Published online: 24 December 2024.
This article is published with open access at AGH University of Science and Technology Journals.

Abstract

The goal of the cooling procedure after austenitizing in the austempering heat treatment process applied to ausferritic ductile iron (ADI) castings is to rapidly reduce the temperature throughout the casting volume to the temperature range of the process window in which the proper metal matrix structure is formed. The lower limit of this range must be higher than the temperature at which the martensitic transformation starts. The upper limit is selected to eliminate the possibility of diffusion decomposition of austenite while holding castings at austempering temperature. Most often in heat treatment practice, salt baths are used for this purpose. Such a solution makes it possible to realize in one device both the procedure of cooling down to a given temperature and the procedure of isothermal heat treatment at this temperature. Unfortunately, the presence of molten salt in the process equipment has a very unfavorable impact on working conditions and ecology. The purpose of this research is to analyze the possibility of replacing the salt bath cooling procedure in the manufacturing process of ADI castings with a water mist spray cooling procedure on the surfaces of the heat-treated casting. If such cooling is effective, subsequent procedures of heat treatment operations can be carried out with traditional furnace equipment without the use of molten salt, which will clearly improve the environmental performance of the enterprise. The article, using analytical and numerical methods, analyzes the possibility of cooling objects made of cast iron with the help of a high-efficiency heat receiver such as water mist spraying. The limiting conditions for carrying out the process for the assumed cooling curve were considered. It was proposed to use a PID controller realizing the function of controlling the intensity of water mist spray, which corresponds to the intensity of the heat flux received from the heat-treated casting. The theoretical analysis carried out allows us to conclude that water mist cooling according to the assumed cooling curve is practically feasible.

Keywords:

Austempered Ductile Iron, quench, PID controller, system identification, digital control system

1. RESEARCH CONTRIBUTION

ADI cast iron combines unique properties: on the one hand, it has very good ductility, and on the other hand, high tensile and wear resistance [1]. These characteristics make it possible to use this type of cast iron as a substitute for alloyed steel or for tempered carburized steel. In addition, the process of obtaining ADI cast iron, although technologically complex, is characterized by relatively low production costs for components. Components made from this material are characterized by extended service life.

To obtain ADI cast iron, ductile iron must be subjected to a specialized heat treatment that involves holding the starting material at a high temperature of 950–815°C (to austenitize the matrix), and then quickly cooled to 450–250°C. At this temperature, a process called isothermal hardening takes place. After its completion, the workpiece is cooled to ambient temperature. The most important and simultaneously most

sensitive stage of processing is the cooling process from the austenitizing temperature to the isothermal hardening temperature. In industrial practice, salt baths are used to ensure an adequate cooling rate in the isothermal hardening process. Most commonly, mixtures of sodium nitrite and potassium nitrate are used for this purpose. However, it should be noted that salts decompose at temperatures of 380–400°C. The compounds released as a result of this decomposition are highly reactive and cause environmental pollution.

The works [2, 3] propose the use of fluidized beds as a method of cooling heat-treated parts. Such a solution, compared to a salt bath, is not harmful to the environment. These works highlight the difficulty of obtaining adequate heat transfer. In the production of ADI castings, attempts were also made to cool using an oil bath; however, the oils used could operate at temperatures no higher than 240°C. Publications [4–8] consider cooling using water mist. It is a highly desirable high heat transfer coefficient medium and environmentally friendly.

The problem with such cooling for ADI isothermal quenching is the danger of obtaining too low a temperature on the surface of the heat-treated casting, and thus starting a martensitic transformation, which eliminates the possibility of obtaining a subassembly with the desired strength characteristics. This publication examines the possibility of the controlled cooling of cast iron after austenitizing with water mist, with the elimination of the danger of overcooling the surface below the temperature of the onset of martensitic transformation.

2. THEORETICAL BASIS AND ANALYTICAL APPROACH TO THE PROBLEM

Heat treatment to produce ADI cast iron consists of several phases: austenitizing, cooling at an appropriate rate to the isothermal quenching temperature and isothermal quenching. Each of these stages is equally important and determines the structure of the microstructure of the cast iron after treatment, on which the physical and mechanical properties of the castings directly depend. Rapid cooling of the heat-treated casting from the austenitizing temperature must be carried out in such a way as to exclude the possibility of austenite decomposition (pearlite transformation) before the isothermal hardening temperature is reached. Figure 1 shows an example of a TTT diagram for unalloyed cast iron. In this figure, the dashed line indicates the heat treatment process required to obtain ADI cast iron.

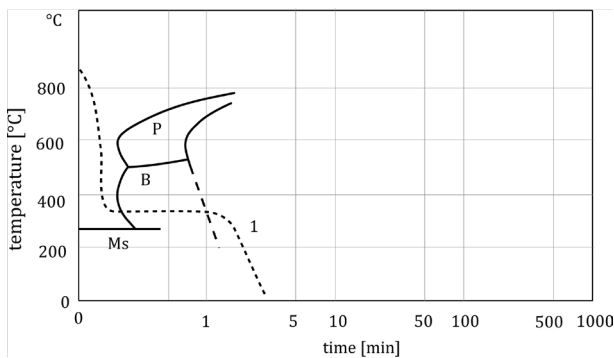


Fig. 1. TTT diagram and flow chart of isothermal hardening of unalloyed cast iron [9]

As shown in Figure 1, after austenitizing annealing, the heat-treated part should be rapidly descended to 270–450°C. For unalloyed cast iron (according to [9]), the cooling time should be a maximum of 15 s. Cooling at this rate for larger wall thickness of the casting is possible only in a layer of limited thickness adjacent to the surface [1]. Determination of the thickness of this layer, among other things, is the subject of ongoing research.

3. ANALYTICAL DETERMINATION OF BOUNDARY CONDITIONS FOR HEAT FLOW IN A HEAT-TREATED MATERIAL (DIRICHLET BOUNDARY CONDITION)

In the first step, we will determine the limiting possibility of heat treatment [10]. The basis of the mathematical analysis is the partial differential equation of thermal conductivity,

which for a one-dimensional space in the absence of internal heat sources takes the form (after transformation from [11]):

$$\frac{\partial u_x}{\partial \tau} = a_m \cdot \left(\frac{\partial^2 u_x}{\partial x^2} \right) \quad (1)$$

where:

$\frac{\partial u_x}{\partial \tau}$ – the rate of change of the temperature of the point x ,
 $\frac{\partial^2 u_x}{\partial x^2}$ – the second spatial derivative of the temperature at x ,

a_m – temperature equalization coefficient (thermal diffusivity) [m^2/s].

The temperature equalization coefficient a_m is defined as:

$$a_m = \frac{\lambda}{c_p \cdot \rho} \quad (2)$$

where:

λ – thermal conductivity coefficient [$\text{W}/(\text{m}\cdot\text{K})$],
 c_p – specific heat [$\text{J}/(\text{kg}\cdot\text{K})$],
 ρ – density [kg/m^3].

Analytical calculations were carried out for a one-dimensional semi-infinite space, while FEM calculations were carried out for a one-dimensional space of finite thickness, but an adiabatic condition was assumed on the other side of the analyzed area. The geometries of the space are shown schematically in Figure 2.

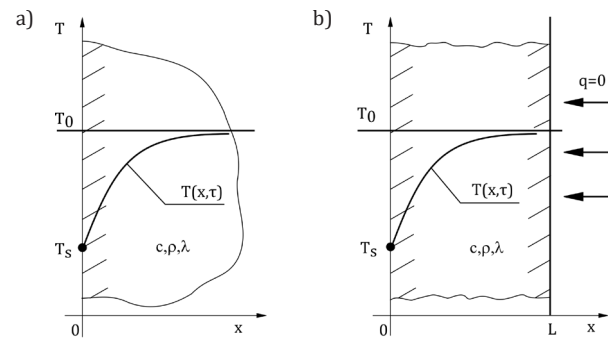


Fig. 2. Geometries of the spaces considered: a) analytical calculations; b) FEM calculations

For the cooled surface, a boundary condition of the first type (Dirichlet boundary condition) was assumed, according to which we set a temperature with a target value on the cooled surface:

$$u(x, \tau)|_{x=0} = T_s = 320^\circ\text{C} \quad (3)$$

The boundary condition for the isolated surface was defined as follows:

$$\left(\frac{du}{dx} \right) |_{x=L} = \dot{q}(x_L, \tau) \rightarrow 0 \quad (4)$$

Initial condition:

$$u(x, \tau)|_{\tau=0} = T_0 = 880^\circ\text{C} \text{ for } x > 0 \quad (5)$$

Taking into account the boundary conditions, a formula was derived to determine the temperature for any distance from the surface and after a certain time.

$$u(x, \tau)|_{x=0} = T_s + (T_0 - T_s) \cdot \operatorname{erf} \left(\frac{x}{2 \cdot \sqrt{a_m \cdot \tau}} \right) \quad (6)$$

where:

$u(x, \tau)$ – temperature at the point x space, in time τ [K],
 x – distance from the surface [m],
 τ – time [s].

4. NUMERICAL DETERMINATION OF BOUNDARY CONDITIONS FOR HEAT FLOW IN A HEAT-TREATED MATERIAL (DIRICHLET BOUNDARY CONDITION)

Numerical calculations were carried out for cast iron with the chemical composition shown in Table 1.

Table 1
Chemical composition of ductile iron used for CCT diagrams and numerical calculations

C	Si	Mn	Ni	Mo
3.29	2.35	0.07	0.94	1.9

For analytical calculations, the following parameters were assumed, invariant over the entire temperature range:

- specific heat 460 [J/(kg·K)],
- density 7200 [kg/m³],
- heat conductivity coefficient: 34 [W/(m·K)].

In the numerical calculations, parameters such as specific heat, density and thermal conductivity coefficient were assumed to be temperature-dependent variables. The temperature dependence of these parameters used in the mathematical modeling is shown in Figure 3.

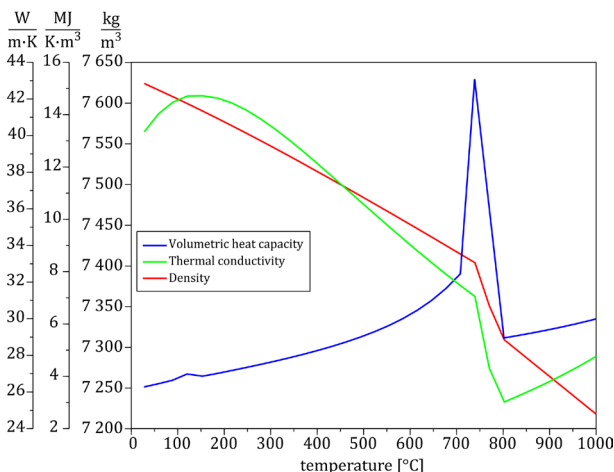


Fig. 3. Volumetric heat capacity, thermal conductivity and density as a function of temperature

These parameters were defined as lookup tables (LUTs) for characteristic temperatures, while intermediate values were calculated by linear approximation of the nearest points. The results of the analytical and numerical calculations are

summarized in Figure 4 in combination with the lines of the CCT diagram for low-alloy cast iron with the elemental contents listed in Table 1 [12]. As can be seen from this figure, obtaining the microstructure characteristic of ADI cast iron (the grade under study) is possible in castings for a layer not exceeding 30 mm in thickness (according to FEM calculations) on the side of the cooled surface.

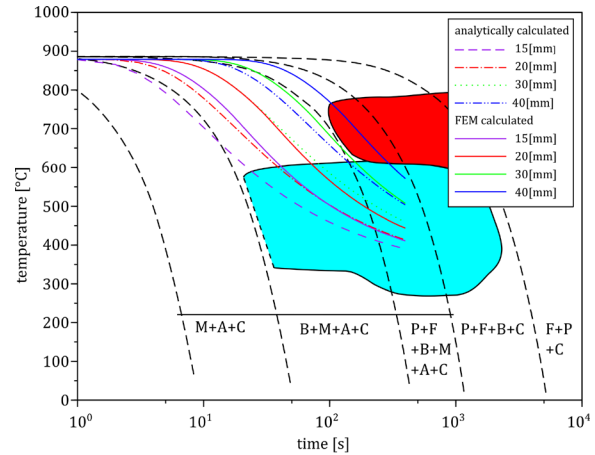


Fig. 4. CCT diagram and cooling curves for isothermal quenching of low-alloy cast iron, for a boundary condition of the first type

Since it is not possible to immediately reach the target temperature at the surface of the cooled wall under practical conditions, the results presented above indicate the theoretical upper limit of the wall thickness, above which it is not possible to ensure an appropriate cooling rate. In what follows, we will consider cooling parameters that satisfy the boundary condition of the third type (Robin boundary condition).

5. NUMERICAL DETERMINATION OF HEAT FLOW CONDITIONS IN THE HEAT-TREATED MATERIAL FOR THE SELECTED COOLING METHOD (ROBIN BOUNDARY CONDITION)

For the numerical calculations, the same parameters were used as in the case of calculations with a Dirichlet boundary condition. The temperature of the cooling medium was set at 20°C. The geometry of the considered space was adopted as in Figure 2b.

Figure 5 shows the different cooling methods and the heat transfer coefficients obtained. It should be noted that according to studies by [13], among others, this coefficient changes with temperature and other parameters. In the temperature range we are interested in, this coefficient is in the range of 2000–8000 W/(m²·K). Two values of the heat transfer coefficient were assumed: 2240 and 7467 W/(m²·K). The choice of such values was dictated by practical considerations and equipment capabilities in the planned research. At this stage of the research, the heat transfer coefficient was assumed to be constant and independent of temperature and other parameters. The adopted values of this coefficient are within the limits reported by other researchers [13–18].

The results of calculating cooling curves for different distances from the cooled surface are shown in Figure 6.

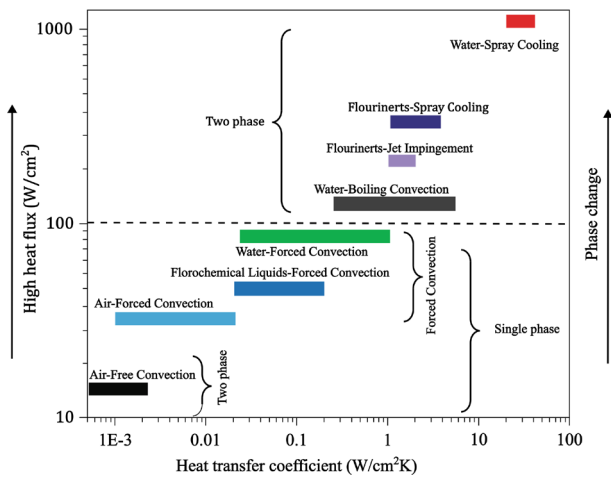


Fig. 5. Comparison of various cooling methods [16]

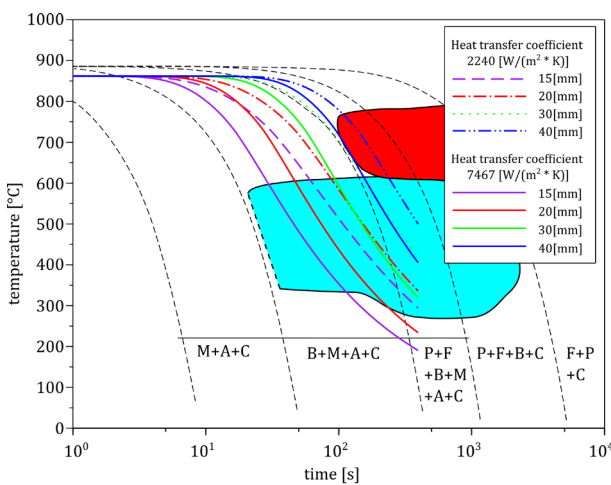


Fig. 6. FEM calculations of temperature changes over time for different distances from the cooled surface and different for different heat transfer coefficients for boundary conditions of the third kind

6. COOLING OF CAST IRON WITH WATER MIST

Analyzing Figure 6 we can deduce that, depending on the value of the actual heat transfer coefficient, we can obtain the cooling rate of the material necessary to obtain the structure characteristic of ADI cast iron in a layer about 30 mm thick for a given cast iron. At the same time, it should be noted that the cooling of the material by spraying water mist, the temperature of which is 20°C, without adequate control of the process will in any case lead to cooling (at least of the surface layer) below the temperature of the onset of martensitic transformation M_s . This means that due to the onset of martensitic transformation, the desired ausferrite microstructure of the matrix will not be obtained. In view of the above, it is necessary to use such a method of cooling control that will ensure an adequate cooling rate and, at the same time, not lead to the undercooling of the material. Thus, it is proposed to use pulsed cooling [8, 19]. The cooling control system will use a feedback loop with surface temperature information processing and a PID controller. Figure 7 shows a calculation scheme for such a designed cooling system.

The main calculation block is the function “Dpole_temp” (bl. 2), which calculates the temperature field in a one-dimensional space using the finite element method. This function takes as input variables including the number of unit elements of the one-dimensional space, the temperature of the cooling medium, the austenitizing temperature and the result of the calculation from block (bl. 1). The computational block (bl. 1) generates a pulse-width modulation waveform (PWM with a period of 1 s), whose signal filling level depends on the error level. The error level is defined as the algebraic sum of the temperature information read at a given distance from the cooled surface and the desired temperature at that distance with a negative sign. Block (bl. 1) simulates pulsed cooling, where control of the average cooling intensity over time is achieved by opening and closing a valve that allows the cooling medium to flow.

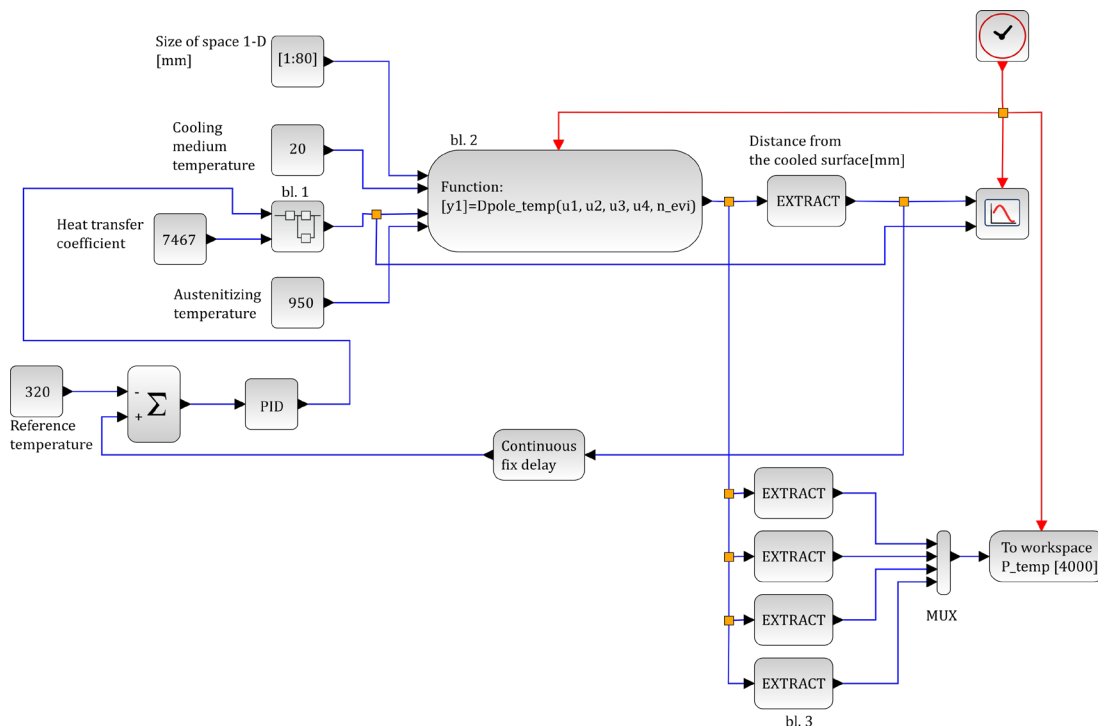


Fig. 7. Calculation scheme of the cooling system

Calculation block bl.3 accumulates temperature information at given distances from the cooling surface. It was assumed in the calculations that, while the surface is not cooled by water mist spray, there is also heat dissipation to the environment resulting from radiation and natural convection – the heat transfer coefficient then takes the value of $100 \text{ W}/(\text{m}^2\cdot\text{K})$.

Figure 8 shows the temperature waveform at a distance of 1 mm from the cooled surface and the waveform of the PWM (Pulse-width modulation) signal implementing the spray control. The temperature change shown in this figure is determined for a heat transfer coefficient of $2240 \text{ W}/(\text{m}^2\cdot\text{K})$.

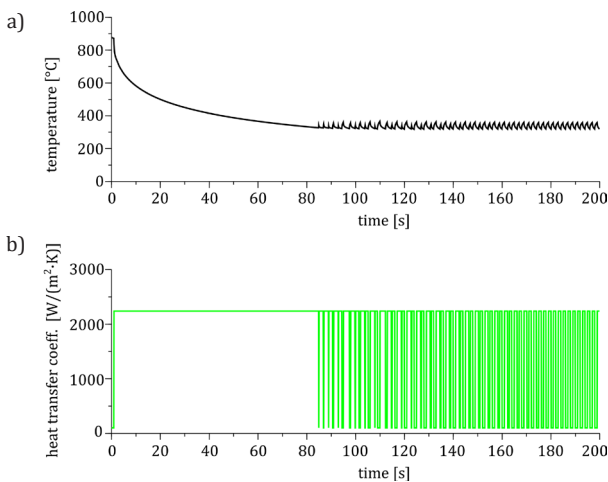


Fig. 8. The course of the water mist cooling process and the corresponding temperature course at a distance of 1 mm from the cooled surface: a) temperature; b) heat transfer coefficient on the cooled surface

As written earlier, the heat transfer coefficients of 2240 and $7467 \text{ W}/(\text{m}^2\cdot\text{K})$ are adopted within the limits set by other researchers [13]. On the other hand, the value of $15000 \text{ W}/(\text{m}^2\cdot\text{K})$ was arbitrarily adopted as a test value for determining the limits of heat treatment capability using PID controller cooling control.

7. CONCLUSIONS

The analytical calculations and numerical simulations of cast iron cooling have shown that we can successfully use pulsed water mist cooling to rapidly cool castings from austenitizing temperature to isothermal hardening temperature during heat treatment of ADI cast iron, eliminating the start of pearlite transformation of austenite without exceeding the temperature of the start of martensitic transformation on the surface of the treated wall. Comparing the results obtained by simulating the cooling controlled by the PID controller and the results of analytical calculations, it can be concluded that by using the PID controller we can achieve a cooling rate comparable with analytical calculations for a boundary condition of the first kind. When simultaneously comparing Figures 9 and 10, it should be noted that a significant increase in the heat transfer coefficient significantly affects the cooling rate in the layers closest to the cooled surface. In layers lying farther from the cooled surface, the physical properties of the heat-treated material begin to play an important role in the rate of temperature change. These properties also have a bearing on the thickness of the layer in which the pearlite transformation will not take place.

As the heat transfer coefficient increases (e.g., by using other spray parameters) due to the nature of spray control (pulse control), the amplitude of temperature spikes in the layers closest to the cooled surface also increases, as illustrated in Figure 11. The effect of the pulsed cooling simulations, among other things, are the cooling curves, which coincide with the cooling curves obtained by calculating the FEM using boundary conditions of the first kind. This may indicate that the achievable boundary values of the cooling rate (at particular distances from the cooled surface) are those derived from calculations using a boundary condition of the first kind.

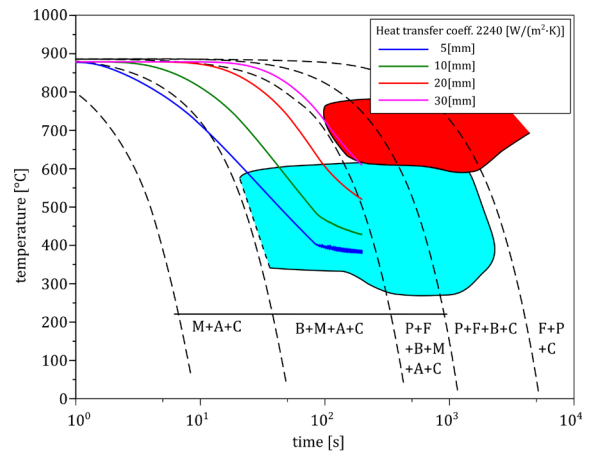


Fig. 9. Cooling curves for heat transfer coefficient $2240 \text{ W}/(\text{m}^2\cdot\text{K})$

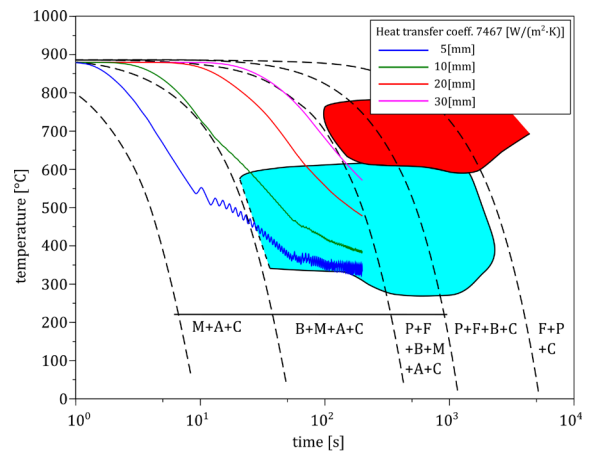


Fig. 10. Cooling curves for heat transfer coefficient $7467 \text{ W}/(\text{m}^2\cdot\text{K})$

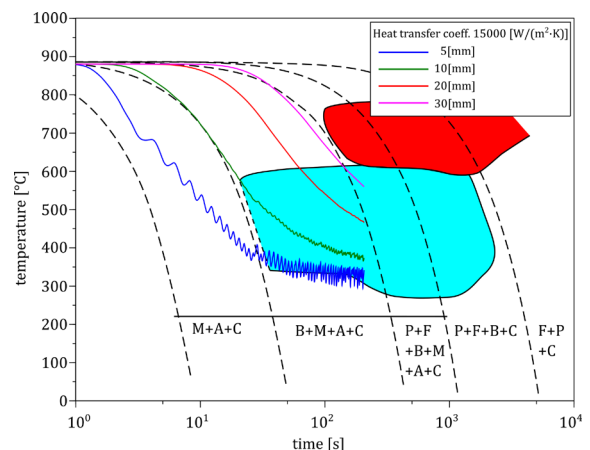


Fig. 11. Cooling curves for heat transfer coefficient $15000 \text{ W}/(\text{m}^2\cdot\text{K})$

REFERENCES

- [1] Ostrowski D., Gumienny G., Sikora M., Kruszyński B. & Pacyniak T. (2015). Obrabialność żeliwa sferoidalnego ADI w procesie szlifowania zewnętrznych powierzchni cylindrycznych. *XXXVIII Naukowa Szkoła Obróbki Ściernej. Łódź – Uniejów*, 262–265. Doi: <https://doi.org/10.17814/mechanik.2015.8-9.381>.
- [2] Mysza D. & Babul T. (2006). Obróbka cieplna żeliwa sferoidalnego w złożach fluidalnych. *Archiwum Odlewnictwa*, 6(20), 177–184.
- [3] Kaczorowski M., Borowski A. & Waszkiewicz S. (1999). Badania struktury i własności żeliwa syntetycznego hartowanego izotermicznie w złożu fluidalnym. *Krzepnięcie Metali i Stopów*, 1(40), 159–164.
- [4] Cebo-Rudnicka A. (2011). *Wpływ warunków chłodzenia oraz przewodności cieplnej wybranych metali na współczynnik wymiany ciepła w procesie chłodzenia z natryskiem wodnym* [doctoral dissertation]. Kraków: Akademia Górniczo-Hutnicza.
- [5] Władysław R. (2008). Water mist effect on heat transfer coefficient in cooling of casting die. *Archives of Foundry Engineering*, 8(3), 227–236.
- [6] Władysław R. (2008). Water mist effect on cooling range and efficiency of casting die. *Archives of Foundry Engineering*, 8(4), 213–218.
- [7] Górny Z., Kluska-Nawarecka S., Czekaj E. & Saja K. (2011). Application of microjet in heat treatment of aluminium bronzes. *Archives of Foundry Engineering*, 11(2), 35–40.
- [8] Czekaj E., Kwak Z. & Garbacz-Klempka A. (2017). Comparison of impact of immersed and micro-jet cooling during quenching on microstructure and mechanical properties of hypoeutectic silumin AlSi7Mg0.3. *Metallurgy and Foundry Engineering*, 43(3), 153–168. Doi: <https://doi.org/10.7494/mafe.2017.43.3.153>.
- [9] Vourinen J., Ingman Y., Johansson M. & Kurkinen M. (1975). Finland Patent No. 377,035. Kuusankoski, Finland
- [10] Mochnacki B. & Suchy J.S. (1993). *Modelowanie i symulacja krzepnięcia odlewów*. Warszawa: Państwowe Wydawnictwo Naukowe PWN.
- [11] Burelko A.A. (2018). *Modelowanie komputerowe krystalizacji odlewów w skali makro i mikro*. Katowice – Gliwice: Wydawnictwo Komisji Odlewnictwa PAN.
- [12] Mrzygłód B., Kluska-Nawarecka S., Kowalski A. & Wilk-Kołodziejczyk D. (2013). Wykorzystanie wykresów CTP niskostopowego żeliwa sferoidalnego do opracowania technologii wytwarzania żeliwa ADI. *Prace Instytutu Odlewnictwa*, 53(4), 85–111. Doi: <https://doi.org/10.7356/iod.2013.24>.
- [13] Jasiewicz E., Hadała B., Cebo-Rudnicka A., Malinowski Z. & Jasiewicz K. (2023). Comparison of the heat transfer efficiency of selected water cooling systems. *15th International Conference on Heat Transfer, Fluid Mechanics and Thermodynamics: Virtual conference, 26–28 July 2021. Proceedings*, 493–498. Doi: <https://doi.org/10.2139/ssrn.4333923>.
- [14] Hnizdil M., Chabicovsky M., Raudensky M. & Lee T.-W. (2016). Heat transfer during spray cooling of flat surfaces with water at large Reynolds numbers. *Journal of Flow Control, Measurement & Visualization*, 4(3), 104–113. Doi: <https://doi.org/10.4236/jfcmv.2016.43010>.
- [15] Leocadio H., van der Geld C.W.M. & Passos J.C. (2019). Heat transfer coefficient during water jet cooling of high temperature steel. *Technical contribution to the 11th International Rolling Conference*. São Paulo, Brasil. Doi: <https://doi.org/10.5151/9785-9785-32400>.
- [16] Xuan Gao & Ri Li (2018). Spray impingement cooling: The state of the art. In: S.M. Sohel Murshed, *Advanced Cooling Technologies and Applications*. Doi: <https://doi.org/10.5772/intechopen.80256>
- [17] Sabariman S., Fang Y. & Specht E. (2016). Analytical and experimental describing the heat transfer in metal quenching with water sprays and jets. *12th International Conference on Heat Transfer, Fluid Mechanics and Thermodynamics*. Costa del Sol, Malaga, Spain.
- [18] Chabičovský M. & Horský J. (2017). Factors influencing spray cooling of hot steel surfaces. In: *Sborník conference METAL 2017*. Ostrava: Tanger, 77–83.
- [19] Tomasik M., Lis S. & Korenko M. (2017). Modulación szerokości impulsu PWM w sterowaniu automatycznym. *Przegląd Elektrotechniczny*, 93(12), 175–178. Doi: <https://doi.org/10.15199/48.2017.12.44>.